



Linseed oil attenuates fatty liver disease in mice fed a high-carbohydrate diet

G. Godoy¹, C.C.O. Bernardo¹, L. Casagrande¹, M.L.M. Sérgio², J.N. Zanoni^{1,2},
J.V.C.M. Perles^{1,2}, R. Curi^{3,4}, and R.B. Bazotte^{1,5}✉

¹Programa de Pós-graduação em Ciências Farmacêuticas, Universidade Estadual de Maringá, Maringá, PR, Brasil

²Departamento de Ciências Morfológicas, Universidade Estadual de Maringá, Maringá, PR, Brasil

³Programa de Pós-graduação Interdisciplinar em Ciências da Saúde, Universidade Cruzeiro do Sul, São Paulo, SP, Brasil

⁴Seção de Produção de Imunobiológicos, Centro Bioindustrial, Instituto Butantan, São Paulo, SP, Brasil

⁵Departamento de Farmacologia e Terapêutica, Universidade Estadual de Maringá, Maringá, PR, Brasil

Abstract

The impact of linseed oil as a lipid source on liver disease induced by a high-carbohydrate diet (HCD) was evaluated. Adult male Swiss mice received an HCD containing carbohydrates (72.1%), proteins (14.2%), and lipids (4.0%). The Control HCD group (HCD-C) received an HCD containing lard (3.6%) and soybean oil (0.4%) as lipid sources. The L10 and L100 groups received an HCD with 10 and 100% linseed oil as lipid sources, respectively. A group of mice were euthanized before receiving the diets (day 0) and the remaining groups after 56 days of receiving the diets (HCD-C, L10, and L-100 groups). Morphological and histopathological analyses, as well as collagen deposition were evaluated. Perivenous hepatocytes (PVH) of the HCD-C group were larger ($P < 0.05$) than periportal hepatocytes (PPH) in the median lobe (ML) and left lobe (LL). There was a greater ($P < 0.05$) deposition of type I collagen in PPH (vs PVH) and in the ML (vs LL). The ML exhibited a higher proportion of apoptotic bodies, inflammatory infiltrate, and hepatocellular ballooning. All these alterations (hepatocyte size, deposition of type I collagen, apoptotic bodies, inflammatory infiltrate, and hepatocellular ballooning) induced by HCD were prevented or attenuated in L10 and L100 groups. Another indicator of the beneficial effects of linseed oil was the lower ($P < 0.05$) number of binucleated hepatocytes (HCD-C vs L10 or L100 group). In general, the L100 group had greater effects than the L10 group. In conclusion, linseed oil impedes or reduces the liver injury progression induced by an HCD.

Key words: Flaxseed oil; Omega 3 polyunsaturated fatty acids; Liver fibrosis; Hepatocellular ballooning; Hepatic steatosis; NAFLD

Introduction

Non-alcoholic fatty liver disease (NAFLD), defined by the excessive accumulation of fatty acids (FA) in the liver (1,2), represents the hepatic manifestation of a metabolic syndrome (3). The progression of NAFLD includes reversible lipid accumulation, non-reversible non-alcoholic steatohepatitis (NASH), which is associated with inflammation and discrete fibrosis process, and aggressive non-reversible cirrhosis, which is characterized by inflammation, consolidation of the fibrotic process, and liver failure (4). The investigation of NAFLD progression includes morphological evaluation, histopathological analysis, and quantification of biomarkers for inflammation and the fibrotic process (5).

High-carbohydrate diets (HCD) lead to the development of NAFLD by increasing FA accumulation in the liver (6). We have investigated the impact of an HCD on FA deposition and composition and inflammation in liver (7),

skeletal muscle (8), brain (9), prefrontal cortex and hippocampus (10), and adipose tissue (11). Additionally, we have examined its effects on systemic inflammation (12,13). Our findings demonstrated that the replacement of conventional lipid sources with canola oil does not prevent HCD-promoted liver FA deposition and inflammation (14). Furthermore, we have reported that the myristic acid:docosahexaenoic acid ratio is a better biomarker of liver inflammation than the omega 6:omega 3 polyunsaturated FA (PUFA) ratio (15).

There is currently no specific treatment for NAFLD progression. The strategies employed include body weight loss and the administration of drugs that decrease insulin resistance (16–18). Linseed oil, a rich source of alpha-linolenic acid, has been reported to benefit cardiovascular diseases, renal diseases, diabetes, and NAFLD (19–22). For instance, Rezaei et al. (23) reported an association

Correspondence: R.B. Bazotte: <rbbazotte@gmail.com>

Received June 7, 2023 | Accepted July 27, 2023

between linseed oil consumption and a reduction in liver FA in NAFLD patients. Linseed oil intake has also been shown to prevent NAFLD induced by a Western-type diet (24).

Recently, we demonstrated that increased inflammation, higher FA deposition, and increased lipid-occupied area in periportal hepatocytes (PPH) and perivenous hepatocytes (PVH) induced by HCD were prevented or attenuated by linseed oil as 10% (L10) or 100% (L100) of the lipid source (5). In this study, we expand upon these findings by assessing the impact of L10 and L100 on liver injury induced by HCD in PVH and PPH of the medium lobe (ML) and left lobe (LL). Additionally, new parameters of liver injury, including inflammation, ballooning, apoptosis, and fibrosis, were included in this study.

Material and Methods

Animals and experimental protocol

Male Swiss mice (*Mus musculus*) from the State University of Maringá Breeding Center (Brazil) were used. Mice weighing approximately 35 g (six weeks old) were housed in a room with controlled temperature ($23 \pm 1^\circ\text{C}$), humidity ($65 \pm 10\%$), and a 12-h light/dark cycle. The experimental protocol (3105210717) was approved by the Animal Ethics Committee of the State University of Maringá.

Before starting the experimental diets, all mice had free access to a standard rodent chow (QuimtiaTM, Brazil). After a 3-day of acclimatization period, the mice were randomly divided into three groups. The groups received a diet consisting of carbohydrates (72.1%), proteins (14.2%), and lipids (4.0%). The HCD-C (control) group received an HCD containing lard (3.6%) and soybean oil (0.4%) as lipid sources, the L10 group received an HCD containing lard (3.6%) and linseed oil (0.4%) as lipid sources, and the L100 group received an HCD containing only linseed oil (4.0%) as lipid source.

All diets were prepared using highly purified ingredients purchased from RhoosterTM Company (Brazil). Lard was purchased from Sadia/BRFTM (Brazil), soybean oil from CocamarTM (Brazil), and LO (*Linun usitatissimum*) from Vital ÂtmanTM (Brazil).

Based on previous studies (5,7,11,14), we determined that 56 days of the diet is sufficient to induce NAFLD. This period also allows for the evaluation of the preventive or attenuating effects of L10 or L100 (5).

In addition to the HCD-C, L10, and L100 groups, we included a group of mice of the same age (six weeks old) as the other groups that was euthanized before initiating the experimental protocol (day 0). This fourth group served as a reference for the detrimental liver effects of HCD (7,11,14,22) and the potential beneficial impact of L10 and L100, as we have shown previously (5,22).

After 56 days of receiving the diets, the mice of the HCD, L10, and L100 groups were euthanized, and the

median lobe (ML) and left lobe (LL) of the liver were sectioned and collected.

Histological analysis

The ML and LL were washed in saline and then fixed in Bouin solution. After six hours, liver samples were dehydrated in a series of increasing alcohol concentration solutions, diaphanized in xylene, and embedded in paraffin. Slices were obtained using a microtome (LeicaTM RM2125 RTS, Germany), and semi-serial sections of 5- μm thickness were mounted on glass. Standard histological analysis was performed using hematoxylin and eosin staining, while Picrosirius staining was used for measuring type I and III collagen.

For the morphometric evaluation of the portal triad and centrilobular vein, images captured with a 40 \times objective were used to select the fields of PPH and PVH (10 hepatocytes per image, 10 images per mouse, 8–10 mice per group). Fields with only hepatocytes and no other structures were selected for hepatocyte quantification (10 images per mouse and 8–10 mice per group). The images were captured using the optical microscope MoticTM BA 400 (Motic China Co, China) with a MoticamTM 2500 5.0 Mega Pixel camera (Motic China Co). Image Pro-PlusTM 4.0 software (Brazil) was used for morphometric analysis and quantification of hepatocytes.

For morphometric measurement of each image, the nuclear and cellular areas (μm^2) were measured in hepatocytes with a visible cytoplasmic membrane, and then the cytoplasmic area (μm^2) for each image was calculated using Image Pro-PlusTM 4.0 software for each image. For hepatocyte quantification, a grid with 336 equidistant points 50 μm apart was overlaid on each image, and only mononucleated and binucleated hepatocytes with nuclei entirely within the grid were counted (Figure 1).

Histopathological analysis was performed on the same slices stained with hematoxylin and eosin under a 20 \times objective. The slices were divided into four quadrants, and the presence and intensity of the apoptotic bodies, inflammatory infiltrate, and hepatocellular ballooning were analyzed in each quadrant. Scores were assigned as follows: score 1: <5 fields, score 2: 6–10 fields, score 3: ≥ 11 fields; score 0: zero fields in the quadrant with apoptotic bodies, inflammatory infiltrate, and hepatocellular ballooning contents. The number of scores in the slice were summed, and then the slices were analyzed for each animal. The maximum score was 60 and the grade of apoptotic bodies, inflammatory infiltrate, and hepatocellular ballooning contents were classified as follows: 0–20 mild-grade; 21–40 moderate-grade; 41–60 severe-grade categories (Figure 2).

Collagen measurement was performed by Picrosirius staining in 5 slices from each mouse. Images were captured with a 20 \times objective on an OlympusTM BX-53 optical microscope (Olympus Co., Japan) with a Roper Scientific PhotometricsTM digital camera (Roper Scientific,

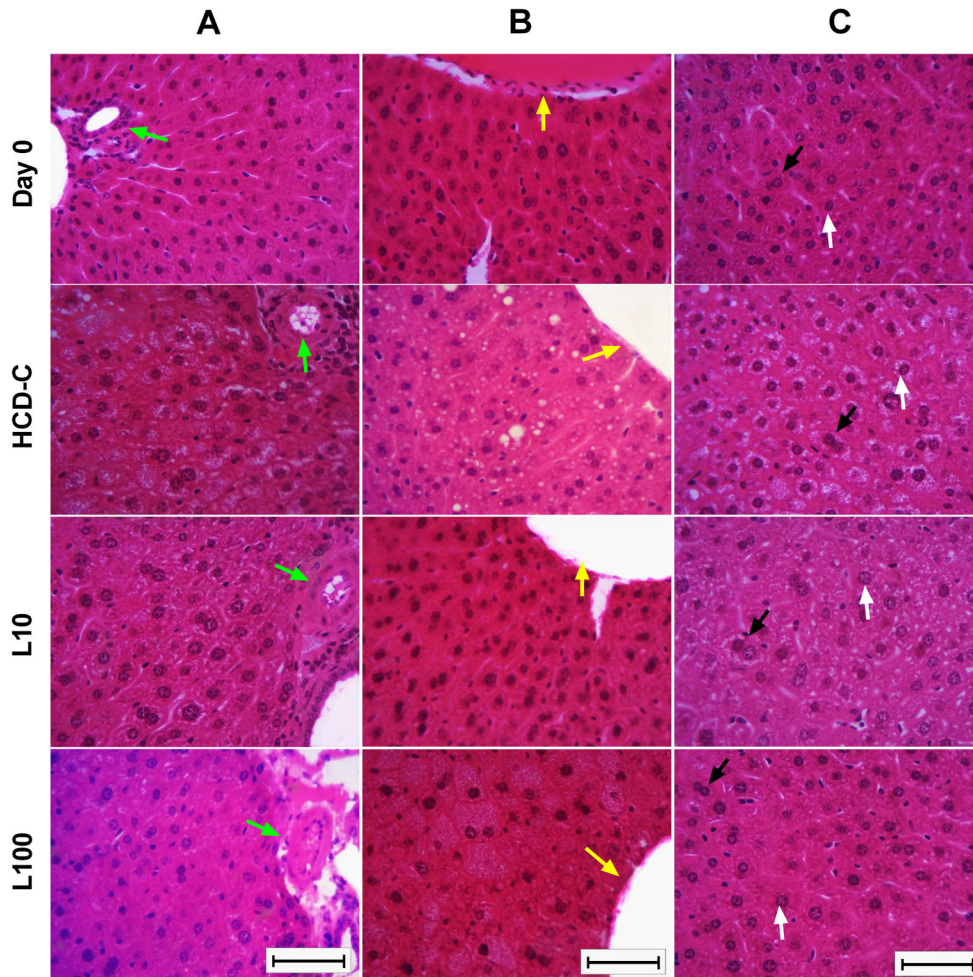


Figure 1. Representative photomicrographs of hematoxylin and eosin staining for quantification and morphometric analysis of hepatocytes obtained from periportal area (portal triad) (A), perivenous area (centrilobular vein) (B), and a clean field (C). The green arrows indicate the hepatic artery branch of the portal triad; the yellow arrows indicate the centrilobular vein branch; the white arrows indicate a mononucleated hepatocyte; the black arrows indicate a binucleated hepatocyte. The evaluations were done before (Day 0) and 56 days after starting the diets (high-carbohydrate diet-control (HCD-C), linseed 10% (L10), or linseed 100% (L100)). The diet of each group is described in the Materials and Methods section. Scale bar: 50 μ m.

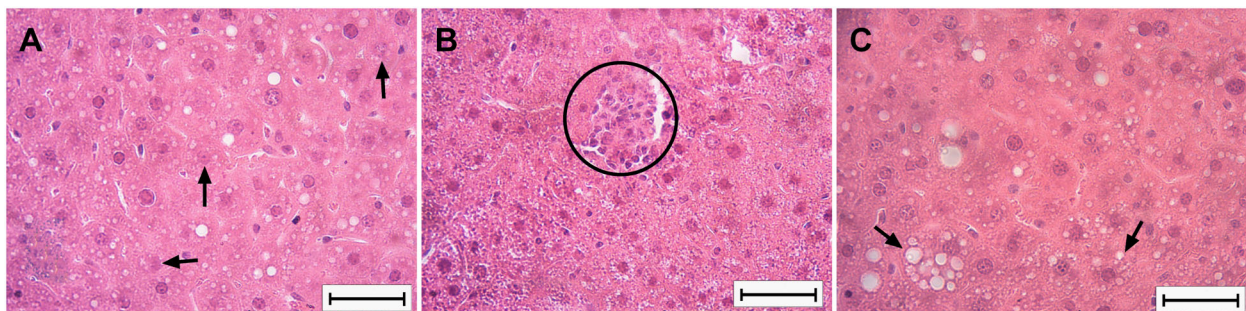


Figure 2. Representative photomicrographs of the histopathological analysis in hematoxylin and eosin staining in the liver. The black arrows indicate apoptotic bodies (A). The black circle marks inflammatory infiltrate (B). The black arrows indicate hepatocellular ballooning (C). Scale bar: 50 μ m.

Table 1. Hepatocyte, nuclei, and cytoplasmic areas of periportal and perivenous hepatocytes.

Parameters	Periportal hepatocytes							
	Day 0 group		HCD-C group		L10 group		L100 group	
	ML	LL	ML	LL	ML	LL	ML	LL
Hepatocyte area (μm^2)	110.88 ±	105.18 ±	98.10 ±	96.05 ±	143.06 ±	137.94 ±	114.80 ±	115.43 ±
	0.82	0.83 ^d	0.81 ^a	1.04 ^a	1.49 ^{ab}	1.41 ^{abd}	0.99 ^{abc}	0.97 ^{abc}
Nuclei area (μm^2)	23.02 ±	22.47 ±	19.50 ±	21.04 ±	28.409 ±	25.99 ±	22.87 ±	22.65 ±
	0.23	0.23	0.23 ^a	0.30 ^{ad}	0.34 ^{ab}	0.32 ^{abd}	0.26 ^{bc}	0.25 ^{bc}
Cytoplasmic area (μm^2)	87.86 ±	82.71 ±	78.61 ±	75.00 ±	114.65 ±	111.95 ±	88.98 ±	92.77 ±
	0.73	0.70 ^d	0.69 ^a	0.84 ^{ad}	1.27 ^{ab}	1.22 ^{ab}	0.81 ^{bc}	0.83 ^{abcd}
	Perivenous hepatocytes							
	Day 0 group		HCD-C group		L10 group		L100 group	
	ML	LL	ML	LL	ML	LL	ML	LL
Hepatocyte area (μm^2)	106.69 ±	103.42 ±	121.21 ±	134.39 ±	121.25 ±	116.58 ±	113.19 ±	120.05 ±
	0.70	0.80 ^d	1.08 ^a	1.47 ^{ad}	1.00 ^a	0.98 ^{abd}	0.87 ^{abc}	1.03 ^{abcd}
Nuclei area (μm^2)	24.17 ±	24.05 ±	24.99 ±	25.86 ±	25.71 ±	25.68 ±	25.84 ±	25.02 ±
	0.25	0.27	0.31 ^a	0.36 ^a	0.31 ^a	0.33 ^a	0.29 ^{abc}	0.29 ^{ad}
Cytoplasmic area (μm^2)	82.51 ±	79.37 ±	96.21 ±	108.53 ±	95.54 ±	90.89 ±	87.35 ±	95.03 ±
	0.55	0.61 ^d	0.87 ^a	1.22 ^{ad}	0.81 ^a	0.74 ^{abd}	0.71 ^{abc}	0.83 ^{abcd}

The evaluations were done before (Day 0) and 56 days after starting the diets (HCD-C: high-carbohydrate diet-control; L10: 10% linseed; L100: 100% linseed). The comparisons were done in the median lobe (ML) and left lobe (LL). Data are reported as means \pm SE of 8–10 mice. ^aP < 0.05 vs Day 0 in the same lobe; ^bP < 0.05 vs HCD-C in the same lobe; ^cP < 0.05 vs L10 in the same lobe; ^dP < 0.05 vs ML in the same group (ANOVA).

Germany) and an OlympusTM light polarizer (Olympus Co.). The centrilobular vein or portal triad in the center (10 images per mouse, 8–10 mice per group) was used as a criterion for selecting the fields for comparison. Image Pro-PlusTM 4.0 software (Media Cybernetics Inc., USA) was used to calculate the percentage of the area occupied by type I (red fibers) or type III collagen (green fibers) in each image, relative to the total size of the image.

Statistical analysis

The data were analyzed using a block design followed by Fisher's test using StatisticaTM 8.0 software (StatSoft, Germany; <https://www.statistica.com>). Differences with P-values < 0.05 were considered statistically significant.

Results

Morphometric analysis

The HCD-C group exhibited smaller ($P < 0.05$) hepatocyte area, nuclei area, and cytoplasmic area in the PPH of ML and LL compared to Day 0 group ($P < 0.05$). In addition, mice receiving HCD enriched with LO 10% (L10 group) or LO 100% (L100 group) had larger ($P < 0.05$) hepatocyte area, nuclei area, and cytoplasmic area in the PPH of ML and LL (HCD-C group vs L-10 group or HCD-C

group vs L-100 group). Furthermore, the L10 group had larger ($P < 0.05$) hepatocyte area, nuclei area, and cytoplasmic area in the PPH of ML and LL compared to the L100 group (Table 1).

Mice receiving HCD enriched with 10% LO (L10 group) or 100% LO (L100 group) showed smaller ($P < 0.05$) hepatocyte and cytoplasmic areas in the PVH of LL (HCD-C group vs L10 group or HCD-C group vs L100 group). For ML, a smaller ($P < 0.05$) hepatocyte area and cytoplasmic area of PVH occurred only in the L100 group (HCD-C group vs L100 group). Additionally, the L10 group had higher ($P < 0.05$) and lower ($P < 0.05$) hepatocyte and cytoplasmic areas in the PVH of the ML and LL, respectively, than the L100 group (Table 1).

The results shown in the Table 1 were rearranged for a better understanding of the impact of HCD and the effect of LO incorporation in the HCD on PPH and PVH of the ML and LL.

On day 0, in the ML, the hepatocyte and cytoplasmic areas of the PPH were greater ($P < 0.05$) than the PVH, whereas the nuclei area of the PVH was higher ($P < 0.05$) than the PPH. Also, on day 0, in LL, the cytoplasmic area of the PPH was greater ($P < 0.05$) than the PVH, whereas the nuclei area of the PPH was smaller ($P < 0.05$) than the PVH (Table 2).

Table 2. Hepatocyte, nuclei, and cytoplasmic areas of cells from the median lobe and left lobe.

Parameters	Median lobe							
	Day 0 group		HCD-C group		L10 group		L100 group	
	PPH	PVH	PPH	PVH	PPH	PVH	PPH	PVH
Hepatocyte area (μm^2)	110.88 \pm 0.82	106.69 \pm 0.70 ^d	98.10 \pm 0.81	121.21 \pm 1.08 ^d	143.06 \pm 1.49	121.25 \pm 1.00 ^d	114.80 \pm 0.99	113.19 \pm 0.87
Nuclei area (μm^2)	23.02 \pm 0.23	24.17 \pm 0.25 ^d	19.50 \pm 0.23	24.99 \pm 0.31 ^d	28.409 \pm 0.34	25.71 \pm 0.31 ^d	22.87 \pm 0.26	25.84 \pm 0.29 ^d
Cytoplasmic area (μm^2)	87.86 \pm 0.73	82.51 \pm 0.55 ^d	78.61 \pm 0.69	96.21 \pm 0.87 ^d	114.65 \pm 1.27	95.54 \pm 0.81 ^d	88.98 \pm 0.81	87.35 \pm 0.71
	Left lobe							
	Day 0 group		HCD-C group		L10 group		L100 group	
	PPH	PVH	PPH	PVH	PPH	PVH	PPH	PVH
Hepatocyte area (μm^2)	105.18 \pm 0.83	103.42 \pm 0.80	96.05 \pm 1.04	134.39 \pm 1.47 ^d	137.94 \pm 1.41	116.58 \pm 0.98 ^d	115.43 \pm 0.97	120.05 \pm 1.03 ^d
Nuclei area (μm^2)	22.47 \pm 0.23	24.05 \pm 0.27 ^d	21.04 \pm 0.30	25.86 \pm 0.36 ^d	25.99 \pm 0.32	25.68 \pm 0.33	22.65 \pm 0.25	25.02 \pm 0.29 ^d
Cytoplasmic area (μm^2)	82.71 \pm 0.70	79.37 \pm 0.61 ^d	75.00 \pm 0.84	108.53 \pm 1.22 ^d	111.95 \pm 1.22	90.89 \pm 0.74 ^d	92.77 \pm 0.83	95.03 \pm 0.83 ^d

The evaluations were done before (Day 0) and 56 days after starting the diets (HCD-C: high-carbohydrate diet-control; L10: 10% linseed; L100: 100% linseed). The comparisons were done between areas of periportal hepatocytes (PPH) and perivenous hepatocytes (PVH). Data are reported as means \pm SE of 8–10 mice. ^d $P < 0.05$ vs PPH in the same group (ANOVA).

The HCD group showed higher ($P < 0.05$) hepatocyte area, nuclei area, and the cytoplasmic area in the PVH than the PPH of the ML and LL (Table 2).

The L10 group exhibited lower ($P < 0.05$) hepatocyte, nuclei, and cytoplasmic areas of PVH than the PPH of the ML. In addition, the L10 group exhibited lower ($P < 0.05$) hepatocyte and cytoplasmic areas of PVH compared to PPH of the LL (Table 2).

The L100 group showed a higher ($P < 0.05$) nuclei area of PVH than PPH in the ML. Also, the L100 group had higher ($P < 0.05$) hepatocyte area, nuclei area, and cytoplasmic area of PVH compared with PPH of the LL (Table 2).

Hepatocyte quantification

The Day 0 group had a lower ($P < 0.05$) amount of mononucleated hepatocytes compared to the HCD-C and L10 groups in the ML. Also, day 0 animals exhibited higher ($P < 0.05$) amounts of binucleated hepatocytes than the L100 animals in the ML and LL.

The HCD-C group showed a higher ($P < 0.05$) amount of mononucleated hepatocytes than the L100 group in the ML and LL. Additionally, the HCD-C group had a higher ($P < 0.05$) amount of binucleated hepatocytes than the L10 and L100 groups the ML and LL.

The L10 group exhibited a higher ($P < 0.05$) amount of mononucleated and binucleated hepatocytes compared to the L100 group in ML.

The L10 group had a higher ($P < 0.05$) number of mononucleated hepatocytes in the ML than LL. Also, the Day 0, HCD-C, and L10 groups exhibited higher ($P < 0.05$) amounts of binucleated hepatocytes in the ML than in LL (Table 3).

Histopathological analysis

The Day 0 group scored practically 100% mild-grade on all parameters in both the ML and LL (Table 4).

The HCD-C presented more moderate-grade and severe-grade scores than the Day 0, L10, and L100 groups in the ML and LL. The ML generally had more moderate-grade and severe-grade scores compared to the LL.

Incorporating LO in the HCD reduced the proportion of apoptotic bodies, inflammatory infiltrate, and hepatocellular ballooning, and the score was moderate instead of severe in the ML and LL.

Collagen measurements

Collagen measurements, reported as a percentage of the occupied area, are described in Figure 3, Table 5, and Table 6. Figure 3 shows the comparison between Day 0, HCD-C, L10, and L100 groups.

For red fibers (type I collagen), the HCD-C, L10, and L100 groups showed a higher percentage ($P < 0.05$) of occupied area compared to the Day 0 group in PPH area of the ML (Figure 3A). The HCD-C group exhibited a higher ($P < 0.05$) percentage of the occupied area compared to the Day 0 group for red fibers in PVH area of the ML (Figure 3B) and LL (Figure 3D). The incorporation of LO in the HCD decreased ($P < 0.05$) the percentage of the occupied area in PVH of the L10 (vs HCD-C) and L100 (vs HCD-C) groups of the ML (Figure 3B) and LL (Figure 3D). In contrast, the incorporation of LO in the HCD increased ($P < 0.05$) the percentage of the occupied area in PPH of the LL in the L10 (vs HCD-C) (Figure 3C). For green fibers (type III collagen), the HCD-C, L10, and

Table 3. Quantification of mononucleated and binucleated hepatocytes (cells/cm²) in the median lobe (ML) and left lobe (LL).

	Day 0 group		HCD-C group		L10 group		L100 group	
	ML	LL	ML	LL	ML	LL	ML	LL
Mononucleated cells	254.1 ± 7.21	252.7 ± 6.85	276.4 ± 7.56 ^a	262.7 ± 7.73	292.3 ± 8.79 ^a	254.5 ± 5.98 ^d	245.3 ± 5.98 ^{bc}	243.3 ± 6.15 ^b
Binucleated cells	230.4 ± 7.56	198.9 ± 9.31 ^d	245.2 ± 10.72	216.5 ± 9.14 ^d	215.1 ± 8.08 ^b	190.0 ± 8.08 ^{bd}	180.1 ± 7.38 ^{abc}	174.2 ± 7.56 ^{ab}

The evaluations were done before (Day 0) and 56 days after starting the diets (HCD-C: high-carbohydrate diet-control; L10: 10% linseed; L100: 100% linseed). ^aP < 0.05 vs Day 0 in the same lobe; ^bP < 0.05 vs HCD-C in the same lobe; ^cP < 0.05 vs L10 in the same lobe; ^dP < 0.05 vs ML in the same group (ANOVA).

Table 4. Histopathological analysis of apoptotic bodies, inflammatory infiltrate, and hepatocellular ballooning in the median and left lobes.

Parameters	Groups	Median lobe		
		Mild-grade (score 0–20) (%)	Moderate-grade (score 21–40) (%)	Severe-grade (score 41–60) (%)
Apoptotic bodies	Day 0	100	0	0
	HCD-C	0	88	12
	L10	71	29	0
	L100	67	33	0
Inflammatory infiltrate	Day 0	100	0	0
	HCD-C	13	62	25
	L10	71	29	0
	L100	67	33	0
Hepatocellular ballooning	Day 0	100	0	0
	HCD-C	0	25	75
	L10	29	0	71
	L100	11	56	33
Left lobe				
Apoptotic bodies	Day 0	100	0	0
	HCD-C	38	50	12
	L10	44	56	0
	L100	80	20	0
Inflammatory infiltrate	Day 0	89	11	0
	HCD-C	13	87	0
	L10	56	44	0
	L100	80	20	0
Hepatocellular ballooning	Day 0	100	0	0
	HCD-C	0	63	37
	L10	0	66	34
	L100	10	50	40

The evaluations were done before (Day 0) and 56 days after starting the diets (HCD-C: high-carbohydrate diet-control; L10: 10% linseed; L100: 100% linseed).

L100 groups showed a lower (P < 0.05) percentage of occupied area compared to Day 0 group in PPH (Figure 3E) and PVH (Figure 3F) of the ML, and PVH of the LL (Figure 3H). In contrast, the incorporation of LO in the HCD increased (P < 0.05) the percentage of occupied area in PPH of the LL in the L10 group (vs HCD-C group) (Figure 3G).

The results of the incorporation of LO in PPH and PPV of the ML and LL (Figure 3A–H) were rearranged in Tables 5 and 6. Table 5 shows the comparison between PPH and PVH, whereas Table 6 shows the comparison between the ML and LL.

For red fibers, the HCD-C, L10, and L100 groups showed a higher (P < 0.05) percentage of the occupied

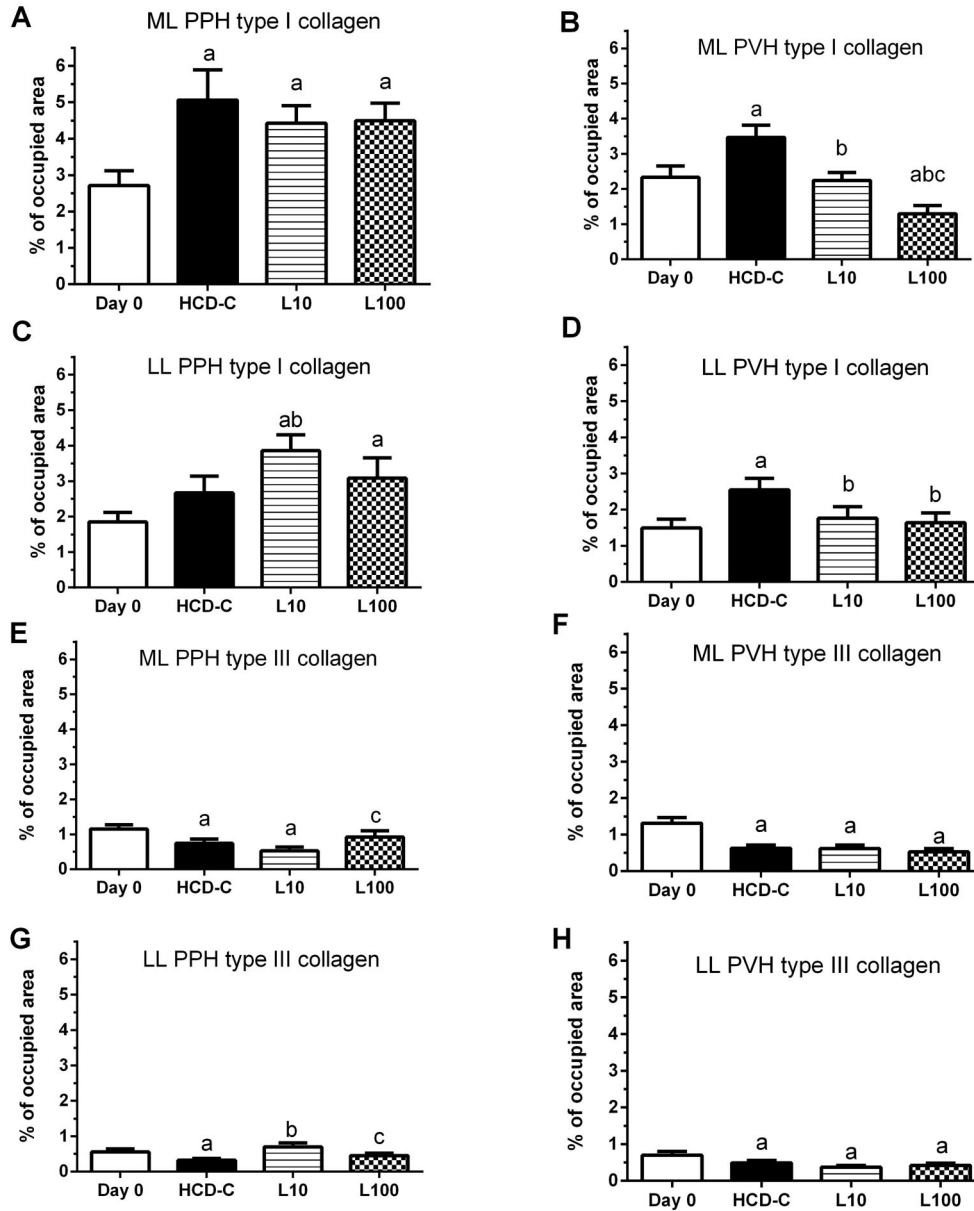


Figure 3. The histograms (A–H) represent the mean percent of occupied area by type I collagen and type III collagen in periportal hepatocytes (PPH) and perivenous hepatocytes (PVH) of the median lobe (ML) and left lobe (LL). The evaluations were done before (Day 0) and 56 days after starting the diets (high-carbohydrate diet-control (HCD-C), linseed 10% (L10), or linseed 100% (L100)). The diet of each group is described in the Materials and Methods section. Data are reported as mean and SD. ^aP < 0.05 vs Day 0; ^bP < 0.05 vs HCD-C (P < 0.05); ^cP < 0.05 vs L10 (ANOVA).

area in PPH than in PVH in the ML. Also for red fibers, L10 and L100 groups showed a higher (P < 0.05) percentage of the occupied area in PPH compared to PVH in the LL (Table 5).

For green fibers, the L10 and L00 groups exhibited a higher (P < 0.05) percentage of the occupied area in PPH compared to PVH in the LL and ML, respectively. The HCD-C

group showed a higher (P < 0.05) percentage of the occupied area in PVH compared to the PPH in the LL (Table 5).

For red fibers, the Day 0, HCD-C, L10, and L100 groups showed a higher (P < 0.05) percentage of the occupied area in the ML than the LL in the PPH and PPV. For green fibers, the Day 0, HCD-C, and L100 groups had a higher (P < 0.05) percentage of the occupied area in the

Table 5. Percentage of area occupied by type I collagen (red fibers) and type III collagen (green fibers) in the median lobe and left lobe.

Collagen	Median lobe							
	Day 0 group		HCD-C group		L10 group		L100 group	
	PPH	PVH	PPH	PVH	PPH	PVH	PPH	PVH
Red fibers	2.33 ± 0.32	2.71 ± 0.40	5.06 ± 0.82	3.47 ± 0.34*	4.42 ± 0.48	2.24 ± 0.22*	4.49 ± 0.48	1.29 ± 0.23*
Green fibers	1.15 ± 0.11	1.31 ± 0.15	0.74 ± 0.11	0.62 ± 0.08	0.52 ± 0.10	0.61 ± 0.09	0.92 ± 0.17	0.52 ± 0.09*
Collagen	Left lobe							
	Day 0 group		HCD-C group		L10 group		L100 group	
	PPH	PVH	PPH	PVH	PPH	PVH	PPH	PVH
Red fibers	1.84 ± 0.27	1.49 ± 0.24	2.66 ± 0.47	2.54 ± 0.32	3.85 ± 0.44	1.76 ± 0.32*	3.08 ± 0.57	1.63 ± 0.27*
Green fibers	0.55 ± 0.08	0.70 ± 0.10	0.32 ± 0.05	0.49 ± 0.06*	0.70 ± 0.10	0.37 ± 0.05*	0.45 ± 0.06	0.41 ± 0.06

The comparisons were done in the periportal hepatocytes (PPH) and perivenous hepatocytes (PVH) before (Day 0) and 56 days after starting the diets (HCD-C: high-carbohydrate diet-control; L10: 10% linseed; L100: 100% linseed). Data are reported as means ± SE of 8–10 mice. *P < 0.05 vs PPH in the same group (ANOVA).

Table 6. Percentage of area occupied by type I collagen (red fibers) and type III collagen (green fibers) in the periportal and perivenous areas.

Collagen	Periportal area							
	Day 0 group		HCD-C group		L10 group		L100 group	
	ML	LL	ML	LL	ML	LL	ML	LL
Red fibers	2.33 ± 0.32	1.84 ± 0.27*	5.06 ± 0.82	2.66 ± 0.47*	4.42 ± 0.48	3.85 ± 0.44	4.49 ± 0.48	3.08 ± 0.57*
Green fibers	1.15 ± 0.11	0.55 ± 0.08*	0.74 ± 0.11	0.32 ± 0.05*	0.52 ± 0.10	0.70 ± 0.10	0.92 ± 0.17	0.45 ± 0.06*
Collagen	Perivenous area							
	Day 0 group		HCD-C group		L10 group		L100 group	
	ML	LL	ML	LL	ML	LL	ML	LL
Red fibers	2.71 ± 0.40	1.49 ± 0.24*	3.47 ± 0.34	2.54 ± 0.32*	2.24 ± 0.22	1.76 ± 0.32*	1.29 ± 0.23	1.63 ± 0.27*
Green fibers	1.31 ± 0.15	0.70 ± 0.10*	0.62 ± 0.08	0.49 ± 0.06	0.61 ± 0.09	0.37 ± 0.05*	0.52 ± 0.09	0.41 ± 0.06

The comparisons were between the median lobe (ML) and left lobe (LL) before (Day 0) and 56 days after starting the diets (HCD-C: high-carbohydrate diet-control; L10: 10% linseed; L100: 100% linseed). Data are reported as means ± SE of 8–10 mice. *P < 0.05 vs median lobes in the same group (ANOVA).

ML than LL in PPH. Also, the Day 0 and L10 groups showed a higher (P < 0.05) percentage of the occupied area in the ML compared to LL in PVH (Table 6).

Discussion

The liver is anatomically divided into lobes, each of which have functional structures known as lobules (25). Since the livers of mice are small and the anatomical division of lobes is not well-defined, we analyzed the ML and LL, which have a larger area, better anatomic position, and lobe division. Considering that liver lobes and lobules are complex structures, it is suggested that

the complex intrahepatic vascular network and oxygen gradient are thought to promote the differentiation between PPH and PVH (26), and an HCD intensifies these differences. For example, PVH of the HCD-C group was larger (vs PPH) not only in the ML but also in the LL. These alterations were prevented or attenuated if the lipid source of the HCD (lard and soybean oil) was replaced by 10% (L10 group) or 100% (L100 group) linseed oil. Similarly, our previous study using the same experimental model (5) demonstrated that the percentage of lipid-occupied area was higher in PVH, while the L10 diet and L100 diet prevented or decreased these alterations.

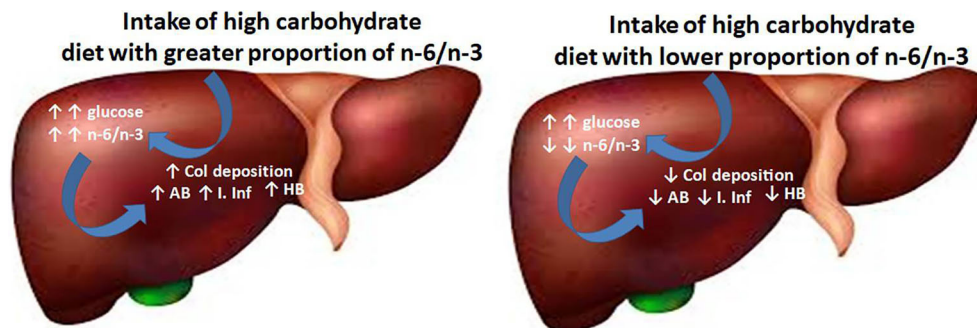


Figure 4. Comparative effects of a high carbohydrate diet (HCD) containing a greater proportion of omega-6:omega-3 polyunsaturated fatty acids (n-6/n-3) and an HCD containing a lower proportion of n-6/n-3. The lower proportion of n-6/n-3 reduces inflammatory infiltrate (I. Inf), collagen 1 (Col) deposition, percent of hepatocellular ballooning (HB), and apoptotic bodies (AB).

Liver fibrosis induced by the HCD was not homogeneous. There was a greater deposition of type I collagen in PPH (vs PVH), probably due to the presence of hepatic stellate cells (HSC) in this region (27). The activation of HSC increases collagen synthesis and promotes fibrosis progression (28–31). HSCs are activated by several factors, including increased lipid accumulation (32,33).

The ML from HCD-C mice exhibited a higher deposition of type I collagen compared to LL. Consistent with these results, the ML showed a higher proportion of apoptotic bodies, inflammatory infiltrate, and hepatocellular ballooning, while in general, linseed oil prevented or attenuated these changes. Apoptotic bodies resulting from the apoptotic process could be triggered by several factors, including FA (34). The inflammatory infiltrate is formed by the recruitment of immune cells during liver injury (35). The higher amount of liver inflammatory infiltrate in the HCD-C group and the lower levels in the animals that received linseed oil in the diet could be associated with the degree of FA deposition, which was higher in the HCD group than in the L10 and L100 groups (5). The mild-grade inflammatory infiltrate in the L100 group could be related to the anti-inflammatory properties of linseed oil (19–24). The presence of severe hepatocellular ballooning confirmed liver injury, which may be caused by the rearrangement of the cytoskeleton (36,37).

Another indicator of the beneficial effects of linseed oil was the lower number of binucleated hepatocytes, an indicator of liver injury (38), in the L10 and L100 groups compared to the HCD-C group.

The morphological and histopathological changes induced by the HCD and the effects of linseed oil showed different degrees of intensity depending on the parameter evaluated, hepatocyte zonation, or lobe localization.

The heterogeneity of liver response to injury opens the possibility of evaluating liver diseases in the entire organ and the morphological and histopathological changes in specific lobes, lobules, and hepatocytes in the portal triad and centrilobular vein.

The L100 diet had more significant effects than the L10 diet. In agreement with this observation, we previously reported that the L100 diet, but not the L10 diet, prevented the elevation of blood triacylglycerol levels promoted by HCD (5).

Additionally, the L100 mice exhibited higher liver levels of omega-3 PUFA and lower levels of saturated FA, monounsaturated FA, and omega-6 PUFA compared to the L10 or HCD-C group, reflecting the higher proportion of omega-3 PUFA in the diet (5).

The beneficial effects of linseed oil demonstrated here and by others (39,40) were not influenced by changes in food intake and body weight (data not shown), as these parameters remained unchanged during the 56 days of experimental diets.

The results described are summarized in Figure 4.

In conclusion, ingestion of linseed oil prevents the progression of liver injury induced by an HCD. These results are relevant considering the absence of pharmacological approaches to prevent NAFLD progression and the difficulties in implementing a long-term weight loss, opening the possibility of using linseed oil as a coadjuvant to prevent or treat liver injury induced by an HCD.

Acknowledgments

The research was supported by the Coordination for the Improvement of Higher Education Personnel (CAPES, Finance Code 001), the Social Demand Grant (No. 88882.448894/2019-01), and CNPq.

References

1. Loomba R, Sanyal AJ. The global NAFLD epidemic. *Nat Rev Gastroentl Hepatol* 2013; 10: 686–690, doi: 10.1038/nrgastro.2013.171.
2. Younossi ZM, Koenig AB, Abdelatif D, Fazel Y, Henry L, Wymer M. Global epidemiology of nonalcoholic fatty liver disease - Meta-analytic assessment of prevalence, incidence, and outcomes. *Hepatology* 2016; 64: 73–84, doi: 10.1002/hep.28431.
3. Vanni E, Bugianesi E, Kotronen A, De Minicis S, Yki-Järvinen H, Sveglia-Baroni G. From the metabolic syndrome to NAFLD or vice versa? *Dig Liver Dis* 2010; 42: 320–330, doi: 10.1016/j.dld.2010.01.016.
4. Kupčová V, Fedelešová M, Bulas J, Kozmonová P, Turecký L. Overview of the pathogenesis, genetic, and non-invasive clinical, biochemical, and scoring methods in the assessment of NAFLD. *Int J Environ Res Public Health* 2019; 16: 3570, doi: 10.3390/ijerph16193570.
5. Godoy G, Antunes MM, Fernandes IDL, Manin LP, Zappiolo C, Masi LN, et al. Linseed oil attenuates liver inflammation, fatty acid accumulation, and lipid distribution in periportal and perivenous hepatocytes induced by a high-carbohydrate diet in mice. *J Med Food* 2022; 25: 1133–1145, doi: 10.1089/jmf.2022.0031.
6. Pompili S, Vetuschi A, Gaudio E, Tessitore A, Capelli R, Alesse E, et al. Long-term abuse of a high-carbohydrate diet is as harmful as a high-fat diet for development and progression of liver injury in a mouse model of NAFLD/NASH. *Nutrition* 2020; 75–76: 111782, doi: 10.1016/j.nut.2020.110782.
7. Silva-Santi LG, Antunes MM, Caparroz-Assef SM, Carbonera F, Masi LN, Curi R, et al. Liver fatty acid composition and inflammation in mice fed with high-carbohydrate diet or high-fat diet. *Nutrients* 2016; 8: 682, doi: 10.3390/nu8110682.
8. Antunes MM, Godoy G, de Almeida-Souza CB, da Rocha BA, da Silva-Santi LG, Masi LN, et al. A high-carbohydrate diet induces greater inflammation than a high-fat diet in mouse skeletal muscle. *Braz J Med Biol Res* 2020; 53: e9039, doi: 10.1590/1414-431x20199039.
9. da Silva-Santi LG, Antunes MM, Mori MA, de Almeida-Souza CB, Visentainer JV, Carbonera F, et al. Brain fatty acid composition and inflammation in mice fed with high-carbohydrate diet or high-fat diet. *Nutrients* 2018; 10: 1277, doi: 10.3390/nu10091277.
10. Antunes MM, Godoy G, Masi LN, Curi R, Bazotte RB. Prefrontal cortex and hippocampus inflammation in mice fed high-carbohydrate or high-fat diets. *J Med Food* 2022; 25: 110–113, doi: 10.1089/jmf.2021.0026.
11. Antunes MM, de Almeida-Souza CB, Godoy G, Crisma AR, Masi LN, Curi R, et al. Adipose tissue is less responsive to food restriction anti-inflammatory effects than liver, muscle, and brain in mice. *Braz J Med Biol Res* 2019; 52: e8150, doi: 10.1590/1414-431x20188150.
12. de Almeida-Souza CB, Antunes MM, Carbonera F, Godoy G, da Silva MARCP, Masi LN, et al. A high-fat diet induces lower systemic inflammation than a high-carbohydrate diet in mice. *Metab Syndr Relat Disord* 2021; 19: 296–304, doi: 10.1089/met.2020.0116.
13. de Almeida-Souza CB, Antunes MM, Godoy G, Schamber CR, Silva MARCP, Bazotte RB. Interleukin-12 as a biomarker of the beneficial effects of food restriction in mice receiving high fat diet or high carbohydrate diet. *Braz J Med Biol Res* 2018; 51: e7900, doi: 10.1590/1414-431x20187900.
14. Antunes MM, Godoy G, Fernandes IDL, Manin LP, Zappiolo C, Masi LN, et al. The dietary replacement of soybean oil by canola oil does not prevent liver fatty acid accumulation and liver inflammation in mice. *Nutrients* 2020; 12: 3667, doi: 10.3390/nu12123667.
15. Antunes MM, Godoy G, Curi R, Visentainer JV, Bazotte RB. The myristic acid:docosahexaenoic acid ratio versus the n-6 polyunsaturated fatty acid:n-3 polyunsaturated fatty acid ratio as nonalcoholic fatty liver disease biomarkers. *Metab Syndr Relat Disord* 2021; 20: 68–79, doi: 10.1089/met.2021.0107.
16. Orci LA, Gariani K, Oldani G, Delaune V, Morel P, Toso C. Exercise-based interventions for nonalcoholic fatty liver disease: a meta-analysis and meta-regression. *Clin Gastroenterol Hepatol* 2016; 14: 1398–1411, doi: 10.1016/j.cgh.2016.04.036.
17. Brunner KT, Henneberg CJ, Wilechansky RM, Long MT. Nonalcoholic fatty liver disease and obesity treatment. *Curr Obes Rep* 2019; 8: 220–228, doi: 10.1007/s13679-019-00345-1.
18. Koutoukidis DA, Astbury NM, Tudor KE, Morris E, Henry JA, Noreik M, et al. Association of weight loss interventions with changes in biomarkers of nonalcoholic fatty liver disease: a systematic review and meta-analysis. *JAMA Intern Med* 2019; 179: 1262–1271, doi: 10.1001/jamainternmed.2019.2248.
19. Goyal A, Sharma V, Upadhyay N, Gill S, Sihag M. Flax and flaxseed oil: an ancient medicine & modern functional food. *J Food Sci Technol* 2014; 51: 1633–1653, doi: 10.1007/s13197-013-1247-9.
20. Zhang X, Wang H, Yin P, Fan H, Sun L, Liu Y. Flaxseed oil ameliorates alcoholic liver disease via anti-inflammation and modulating gut microbiota in mice. *Lipids Health Dis* 2017; 16: 44, doi: 10.1186/s12944-017-0431-8.
21. Candido CJ, Figueiredo PS, Silva RDC, Portugal LC, Jaques JAS, Almeida JA, et al. Protective effect of α -linolenic acid on non-alcoholic hepatic steatosis and interleukin-6 and -10 in wistar rats. *Nutrients* 2019; 12: 9, doi: 10.3390/nu12010009.
22. Barrena HC, Schiavon FPM, Cararra MA, Marques ACR, Schamber CR, Curi R, Bazotte RB. Effect of linseed oil and macadamia oil on metabolic changes induced by high-fat diet in mice. *Cell Biochem Funct* 2014; 32: 333–340, doi: 10.1002/cbf.3018.
23. Rezaei S, Sasani MR, Akhlaghi M, Kohanmoo A. Flaxseed oil in the context of a weight loss programme ameliorates fatty liver grade in patients with non-alcoholic fatty liver disease: a randomised double-blind controlled trial. *Br J Nutr* 2020; 123: 994–1002, doi: 10.1017/S0007114520000318.
24. Han H, Qiu F, Zhao H, Tang H, Li X, Shi D. Dietary flaxseed oil prevents western-type diet-induced nonalcoholic fatty liver disease in apolipoprotein-e knockout mice. *Oxid Med*

- Cell Longev* 2017; 2017: 3256241, doi: 10.1155/2017/2356241.
25. Kruepunga N, Hakvoort TBM, Hikspoors JPJM, Köhler SE, Lamers WH. Anatomy of rodent and human livers: what are the differences? *Biochim Biophys Acta Mol Basis Dis* 2019; 1865: 869–878, doi: 10.1016/j.bbadis.2018.05.019.
 26. Bazotte RB, Silva LG, Schiavon FP. Insulin resistance in the liver: Deficiency or excess of insulin? *Cell Cycle* 2014; 13: 2494–2500, doi: 10.4161/15384101.2014.947750.
 27. Zou Z, Ekataksin W, Wake K. Zonal and regional differences identified from precision mapping of vitamin A-strong lipid droplets of the hepatic Stellate cells in pig liver: A novel concept of addressing the intralobular area of heterogeneity. *Hepatology* 1998; 27: 1098–1108, doi: 10.1002/hep.510270427.
 28. Hou W, Syn WK. Role of metabolism in hepatic stellate cell activation and fibrogenesis. *Front Cell Dev Biol* 2018; 6: 150, doi: 10.3389/fcell.2018.00150.
 29. Khomich O, Ivanov V, Bartosch B. Metabolic hallmarks of hepatic stellate cells in liver fibrosis. *Cells* 2020; 9: 24, doi: 10.3390/cells9010024.
 30. Yan Y, Zeng J, Xing L, Li C. Extra- and intra-cellular mechanisms of hepatic stellate cell activation. *Biomedicines* 2021; 9: 1014, doi: 10.3390/biomedicines9081014.
 31. Bhattacharya A, Dhar P, Mehra RD. Preliminary morphological and biochemical changes in rat liver following postnatal exposure to sodium arsenite. *Anat Cell Biol* 2012; 45: 229–240, doi: 10.5115/acb.2012.45.4.229.
 32. Wobser H, Dorn C, Weiss TS, Amann T, Bollheimer C, Büttner R, et al. Lipid accumulation in hepatocytes induces fibrogenic activation of hepatic stellate cells. *Cell Res* 2009; 19: 996–1005, doi: 10.1038/cr.2009.73.
 33. Lee YS, Kim SY, Ko E, Lee JH, Yi HS, Yoo YJ, et al. Exosomes derived from palmitic acid-treated hepatocytes induce fibrotic activation of hepatic stellate cells. *Sci Rep* 2017; 7: 3710, doi: 10.1038/s41598-017-03389-2.
 34. Guicciardi ME, Malhi H, Mott JL, Gores GJ. Apoptosis and necrosis in the liver. *Compr Physiol* 2013; 3: 977–1010, doi: 10.1002/cphy.
 35. Koyama Y, Brenner DA. Liver inflammation and fibrosis. *J Clin Invest* 2017; 127: 55–64, doi: 10.1172/JCI88881.
 36. Lackner C. Hepatocellular ballooning in nonalcoholic steatohepatitis: the pathologist's perspective. *Expert Rev Gastroenterol Hepatol* 2011; 5: 223–231, doi: 10.1586/egh.11.8.
 37. Caldwell S, Ikura Y, Dias D, Isomoto K, Yabu A, Moskaluk C, et al. Hepatocellular ballooning in NASH. *J Hepatol* 2010; 53: 719–723, doi: 10.1016/j.jhep.2010.04.031.
 38. Grizzi F, Chiriva-Internati M. Human binucleate hepatocytes: Are they a defence during chronic liver diseases? *Med Hypotheses* 2007; 69: 258–261, doi: 10.1016/j.mehy.2006.12.029.
 39. Yari Z, Cheraghpour M, Alavian SM, Hedayati M, Eini-Zinab H, Hekmatdoost A. The efficacy of flaxseed and hesperidin on non-alcoholic fatty liver disease: an open-labeled randomized controlled trial. *Eur J Clin Nutr* 2021; 75: 99–111, doi: 10.1038/s41430-020-0679-3.
 40. Yari Z, Rahimlou M, Eslamparast T, Ebrahimi-Daryani N, Poustchi H, Hekmatdoost A. Flaxseed supplementation in non-alcoholic fatty liver disease: a pilot randomized, open labeled, controlled study. *Int J Food Sci Nutr* 2016; 67: 461–469, doi: 10.3109/09637486.2016.1161011.